International Journal of Current Science Research and Review
ISSN: 2581-8341
Volume 08 Issue 07 July 2025
DOI: 10.47191/ijcsrr/V8-i7-02, Impact Factor: 8.048
IJCSRR @ 2025
www.ijcsrr.org

Biosynthesis of Ag-nanoparticles from North Central Nigerian Propolis Extract as Highly Efficient Anticorrosion Additive of Carbon Steel in Acidic Medium

Godwin Abawulo Ijuo[1*], Pius Oziri Ukoha[2], Nguano Surma[3]
[1,3]Department of Chemistry, Federal University of Agriculture, PMB, 2373, Makurdi, Nigeria.
[2]Department of Pure and Industrial Chemistry, University of Nigeria, Nsukka

ABSTRACT: Metals in use begin to corrode as soon as they come in contact with a hostile environment. This drastically reduces the useful life of metallic materials, affecting home and industrial properties. In addition to the high cost of production, inorganic corrosion inhibitors are known to be harmful to the ecosystem, thus the need for low-cost, efficient, and environmentally friendly alternatives. Due to their high surface-to-volume ratio and capacity to create self-assembled films on metal surfaces, benign nanoparticles present a good alternative. In this study, North Central Nigerian propolis Extracts (NCNPE) were utilized to synthesize silver nanoparticles and were characterized spectroscopically. The North Central Nigerian propolis Extracts-Silver Nanoparticles composites (NCNPE -AgNPs) were then tested for corrosion-inhibitive potentials in HCl solution. The surface plasmon resonance (SPR) absorption bands were obtained at around 422 nm. The XRD results showed that the resultant crystalline NCNPE -AgNPs has FCC structure, with a mean nanoparticle size of 1.36128 ± 0.04962. The STEM image revealed several oval structures that were densely filled with AgNPs, which appeared as white spots, with patterns that appeared homogeneous. In the presence of 1000 ppm NCNPE -AgNPs, the results showed high inhibition efficiency of 86.49 and 96.44 % for EIS and gravimetric technique, respectively. Also, the thermodynamic and adsorption characteristics of NCNPE -AgNPs on CS in HCl solution were calculated. It was discovered that the NCNPE -AgNPs performed well as an inhibitor of CS corrosion in HCl.

KEYWORDS: Synthesis; characterization; nanoparticles; anticorrosion; EIS; gravimetric analysis

1. INTRODUCTION

Carbon steel is the most prevalent metal utilized in industry, constituting approximately 85% of the steel produced annually [1-2]. This indicates that carbon steel is considerably susceptible to corrosion, rendering it one of the most vulnerable metals. Due to their efficacy, cost-effectiveness, and eco-friendliness, organic compounds have increasingly become the preferred alternative to synthetic inhibitors, which have been prohibited due to their harmful effects on human health and the environment [3-5]. The presence of heteroatoms such as nitrogen, oxygen, sulfur, and phosphorus in these compounds facilitates their adhesion to metal surfaces, forming protective films that obstruct active sites and reduce the metal's exposure to environmental factors [6-8].

Propolis possesses a relatively high concentration of flavonoids, which exhibit properties that can function as corrosion inhibitors, including conjugated double bonds, electronegative atoms, and aromatic rings [9-10]. Honeybees produce the resinous substance known as propolis from flowers and leaf buds to act as a sealant for cracks, a smoother for walls, a regulator of temperature and moisture content, and to maintain an aseptic environment within the hive throughout the year. The composition and color of propolis are influenced by various factors, such as the season of collection, the time of its formation, the botanical sources of its components, the hive's location, and the species of bees utilized [11-12]. Most propolis has been found to comprise a combination of waxes, pollen, essential and aromatic oils, and other organic materials, including bee enzymes. Due to its diverse biological properties and applications in medicine, propolis has garnered significant interest from researchers [13].

With certain modifications, corrosion inhibition studies can leverage the exceptional capabilities of nanomaterials to create self-assembling coatings on metal surfaces. Silver nanoparticles are particularly noted for their heightened reactivity in acidic aqueous environments [14–15]. Recent research has demonstrated that composite materials comprised of organic molecules and nanoparticles are highly effective in preventing corrosion of carbon steel under acidic conditions [16–17].

International Journal of Current Science Research and Review
ISSN: 2581-8341
Volume 08 Issue 07 July 2025
DOI: 10.47191/ijcsrr/V8-i7-02, Impact Factor: 8.048
IJCSRR @ 2025
www.ijcsrr.org

2. MATERIALS AND METHODS

To create 6.00 cm^2 surface area coupons, 0.12 cm thick carbon steel (CS) was cut into 3 x 2 cm coupons. The coupon samples underwent polishing, ethanol degreasing, acetone drying, and storage in a desiccator. The corrosive media for the experiment was a 1.0 M solution of hydrochloric acid Reagents of analytical grade were utilized in this experiment. Before usage, the solvents n-hexane, ethyl acetate, and methanol underwent one more distillation. Water that had been twice distilled was used to prepare all the reagents.

2.1. Preparation and extraction of propolis samples.

Samples of propolis were obtained from a bee farmer in Benue, North Central Nigeria. The propolis samples were mashed with a pestle and mortar after being air-dried for two weeks. The 100 g of finely ground materials were first macerated for 72 hours at room temperature to remove fat using n-hexane. The marc was re-extracted using ethyl acetate and methanol after filtration with Whatman No. 1 filter paper using a vacuum pump. A rotating vacuum evaporator was used to extract the solvents from the mixture entirely. Until used, the powdered extracts were then stored in opaque vials at 4 °C.

2.2. Synthesis of propolis silver nanoparticles (NCNPE -AgNPs).

The method used to synthesize NCNPE -AgNPs was identical to that described [18]. Reducing silver nitrate solution in the presence of the propolis extract constituted the basis for producing NCNPE -AgNPs composite. 100 mL of de-ionized water was added to a beaker holding 1.0 g of propolis extract with vigorous shaking for 1 hour. 100 mL of 1.0 mM AgNO3 was then added, and the mixture was stirred at 25 °C for 48 hours. Visual observation of color change was by UV/Vis spectrophotometer. The pellets were collected and stored after centrifuging to separate the produced silver nanoparticles. The supernatant was discarded.

2.3. Characterization of NCNPE -AgNPs.

The spectroscopic evaluation was used to keep track of the bioreduction of silver ions. Using a JENWAY 6405 UV-visible spectrophotometer with a resolution of 0.1 nm, bandwidth of 5 nm, and a scan speed of 1000 nm/min, absorption measurements in the 190-1100 nm range were performed. X-ray Diffractometer Thermo Scientific model: ARL'XTRA goniometer system, with h, k, and l values, was used to conduct the X-ray diffraction (XRD) examination. SEM (Phenom Pro, 800-07334, Netherlands) operating at 15 kV was used to examine the surface morphology of NCNPE -AgNPs. GeminiSem-500-70-18 Scanning Transmission Electron Microscopy was used to conduct additional research on the image and the diffraction pattern (STEM). Fourier Transfer-Infra Red (FT-IR) spectroscopy (Agilent Cary 630 FTIR fitted with ZnSe optics and a DTGS detector) was used to examine the functional groups on the sample.

2.4. Corrosion inhibition test.

2.4.1. Gravimetric measurement.

Pre-weighed CS coupons were submerged in 200 mL of 1.0 M HCl. The NCNPE–AgNPs concentrations utilized in this study ranged from 200, 400, 600, 800, and 1000 ppm. Tests were run for 24, 48, 72, 96, 120, 144, and 168 hours at room temperature. For three hours of immersion duration, the effect of temperature was also tested at 303, 313, 323, and 333 K, respectively. The CS coupons were taken out of the acid-inhibitor system once the immersion period had passed, cleaned, dried, and weighed. The weight loss was taken to be the difference between the coupon's initial and final weight at a particular period. Every test was carried out in duplicate. The inhibition efficiency (%IE) and corrosion rate of mild steel were calculated from the weight loss results, according to equations 1 and 2 [19-20],

$$IE_{\exp} = \left(1 - \frac{W_{(1)}}{W_{(0)}}\right) x100 \qquad 1$$

where, (0) W is the weight loss of the mild steel without inhibitor and (1) W is the weight loss of mild steel with inhibitor.

$$CR\left(gh^{-1}cm^{-2}\right) = \frac{\Delta W}{At} \qquad 2$$

where ΔW is the weight loss, A is the area of the coupon and t is the immersion time.

International Journal of Current Science Research and Review
ISSN: 2581-8341
Volume 08 Issue 07 July 2025
DOI: 10.47191/ijcsrr/V8-i7-02, Impact Factor: 8.048
IJCSRR @ 2025
www.ijcsrr.org

2.4.2. Electrochemical impedance spectroscopy (EIS).

The experiments were conducted at 303 K using 200 mL of test solution. A conventional three-electrode system consisting of CS as a working electrode, an auxiliary electrode, and a reference electrode was used for the measurements. The %IE were calculated from the charge transfer resistance (Rct) values by using the equation:

$$\%IE = \frac{R_{ct} - R_{ct}^{0}}{R_{ct}} \times 100 \qquad 3$$

where, R_{ct}^{0} is the charge transfer resistance of MS without inhibitor and R_{ct} is the charge transfer resistance of CS with inhibitor. The double layer capacitance (C_{dl}) was calculated using equation 4

$$C_{dl} = \frac{1}{2\pi f_{max} R_{ct}} \qquad 4$$

where f_{max} is the frequency at which the imaginary component of impedance is maximum [21].

3.0 RESULT AND DISCUSSION

3.1.1 Characterization of NCNPE-AgNPs

UV-vis absorption spectrum of the synthesized silver nanoparticles with NCNPE-AgNPs are shown as Plate 1. It can be observed from the spectrum of NCNPE-AgNPs that the surface Plasmon resonance band appears at about 420–430 nm, which produced a peak at around 422 nm.

Plate 1: Optical colour change of raw propolis extracts in de-ionized water and the final silver dispersion formed after reduction with 1 mM $AgNO_3$ solution NCNPE-AgNPs

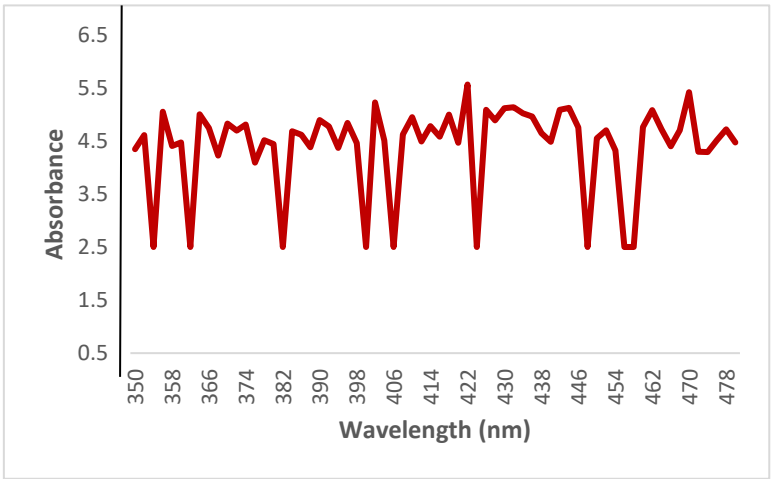

Figure 1: UV-vis absorption spectra of NCNPE-AgNPs

International Journal of Current Science Research and Review
ISSN: 2581-8341
Volume 08 Issue 07 July 2025
DOI: 10.47191/ijcsrr/V8-i7-02, Impact Factor: 8.048
IJCSRR @ 2025
www.ijcsrr.org

3.1.2 XRD Analysis for the Synthesized AgNPs

In the X-ray diffractogram of Ag nanoparticles prepared with NCNPE is shown in Figure 2. The band characteristics of Ag appeared in three peaks, attributed to Ag were present at 2Θ = 38.10 (111), 45.98 (200) and 67.01 (220).

The observed crystallographic planes of the Bragg reflection based on the face-centred cubic structure (fcc) of AgNPs from NCNPE supported crystallinity of the Ag nanoparticles. The average crystallite size as calculated by Scherer's equation (5), was found to be 2.36 nm for NCNPE-AgNPs respectively, [22-23].

$$D = \frac{K\lambda}{\beta Cos\theta} \qquad (5)$$

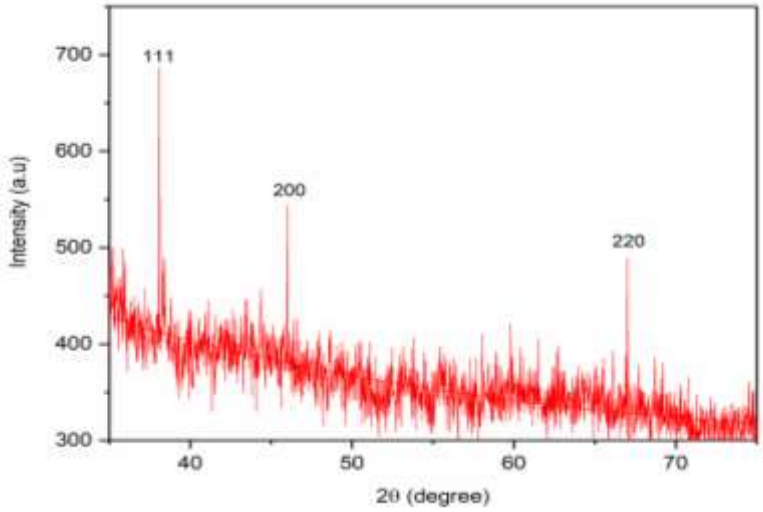

Figure 2: X-ray Diffraction Spectrum of NCNPE-AgNPs

3.1.3 Scanning Electron Microscopy/Energy Dispersive X-Ray (SEM/EDX)

SEM/EDX images of the synthesized NCNPE-AgNPs IN shown in Figure 3. The EDX graphs of NCNPE-AgNPs shows the presence of silver (Ag) and carbon (C), as the major composition of the synthesized nanoparticles. The presence of other elements is probably due to the presence of substrate over which the NP sample was held during SEM microscopy. Figure 4 shows the rain size distribution histogram of silver nanoparticles sizes obtained by means of the SEM result. As can be seen from the distribution, the mean particle size of 1.36128 ± 0.04962 were obtained.

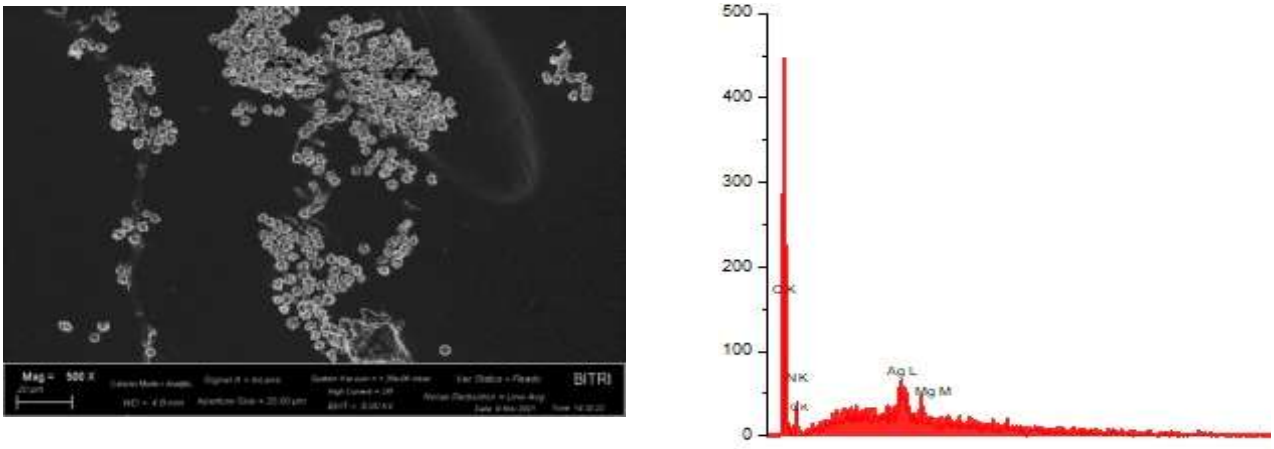

Figure 3: Scanning Electron Microscopy/Energy Dispersive X-Ray (SEM/EDX) of NCNPE-AgNPs

International Journal of Current Science Research and Review
ISSN: 2581-8341
Volume 08 Issue 07 July 2025
DOI: 10.47191/ijcsrr/V8-i7-02, Impact Factor: 8.048
IJCSRR @ 2025
www.ijcsrr.org

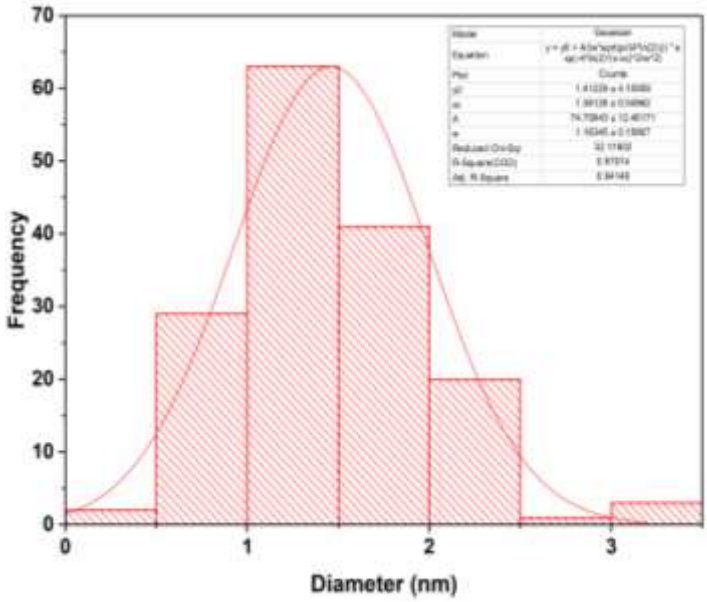

Figure 4: Grain size distribution histogram of silver nanoparticles sizes obtained by means of the SEM result for NCNPE-AgNPs

3.1.4 Scanning Transmission Electron Microscopy (STEM) Analysis for the Synthesized AgNPs

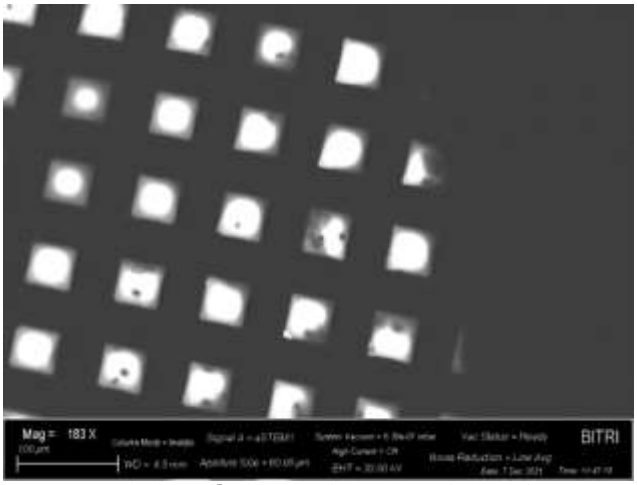

Figure 5: Scanning Transmission Electron Microscopy (STEM) Spectra of NCNPE-AgNPs

The STEM image (Figure 5) revealed several round or oval structures that were densely filled with AgNPs, which appear as black spots with pattern that appeared homogeneous. The degree of overlap of Ag-NPs in these image areas was sufficiently low, such that we could identify and possibly count individual NPs, thus, a homogeneous distribution of the AgNPs throughout the analyzed areas. This distribution points toward localization of the NPs [24-25].

3.2 Corrosion Inhibition Studies

3.2.1 Weight Loss Measurements

Table 1 present the inhibition efficiencies of the inhibitors on CS in 1.0 M HCl calculated from equation 1. It can be seen from the results obtained that the inhibition efficiencies increased with increase in concentration of the inhibitor.

International Journal of Current Science Research and Review
ISSN: 2581-8341
Volume 08 Issue 07 July 2025
DOI: 10.47191/ijcsrr/V8-i7-02, Impact Factor: 8.048
IJCSRR @ 2025
www.ijcsrr.org

The corrosion rates obtained from the analysis in the absence and presence of the inhibitors using equation 2 are shown Figure 6. The corrosion rate was found to decrease with increase in concentration of the inhibitors but increase with time.

Table 1. Effects of Immersion Time and Concentration of NCPNE-AgNPs on the Inhibition efficiencies of CS in 1.0 M HCl

Time (hrs)	Inhibitor Concentration (ppm)					
	Blank	200	400	600	800	1000
24	-	68.77	71.43	73.33	74.07	74.73
48	-	70.74	72.97	75.67	78.01	78.59
72	-	71.63	74.55	76.06	78.32	78.81
96	-	78.33	81.76	83.71	84.32	85.09
120	-	81.44	82.09	87.93	84.43	85.77
144	-	87.83	87.97	89.44	89.67	91.17
168	-	89.67	90.79	91.00	95.06	96.44

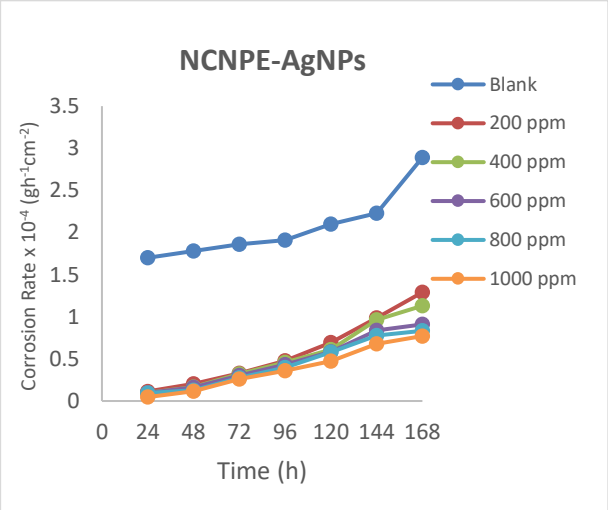

Figure 6: Corrosion rates of CS in 1.0 M HCl in the absence and presence of the various concentration of NCPNE-AgNPs as a function of immersion time (h)

3.2.2: Thermometric Measurements

The values of inhibition efficiencies of the NCNPE-AgNPs on mild steel in 1.0 M HCl from thermometric measurements at 303, 313, 323, 333 and 343 K in the absence and presence of various concentration of the inhibitor are summarized in Table 2. It can be seen from the results obtained that the inhibition efficiencies increase with increase in concentration of the inhibitors but decreased with increase in temperature. Also, the corrosion rates, as shown in Figure 7 were found to increase with temperature.

Table 2: ***Effects of temperature on the the Inhibition efficiencies of CS in 1.0 M HCl in the presence and absence of NCPNE-AgNPs***

Temperature (K)	Inhibitor Concentration (ppm)					
	Blank	200	400	600	800	1000
303	-	60.68	65.09	76.15	82.24	91.63
313	-	58.66	58.93	61.57	63.21	67.67
323	-	57.13	57.11	61.00	62.28	64.54
333	-	54.87	56.56	57.25	59.78	60.47
343	-	47.61	48.10	49.60	50.11	52.55

International Journal of Current Science Research and Review
ISSN: 2581-8341
Volume 08 Issue 07 July 2025
DOI: 10.47191/ijcsrr/V8-i7-02, Impact Factor: 8.048
IJCSRR @ 2025
www.ijcsrr.org

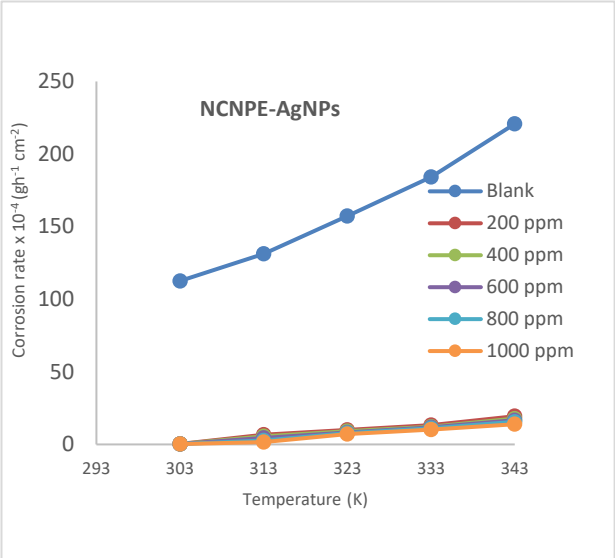

Figure 7: Corrosion rates of mild steel in 1.0 M HCl in the absence and presence of the various concentration of NCNPE-AgNPs as a function of temperature (K)

3.2.3 Electrochemical Analysis

The Nyquist diagrams (Figure 8) are not perfect semicircles, a phenomenon that is referred to as the frequency dispersion of interfacial impedance. This is due to the surface roughness or inhomogeneity of the metal surface associated with solid metal electrodes because of the presence of a non-ideal frequency response for which constant phase element CPE was used [26-27]

The Bode impedance and Bode phase charts for the MS electrode in the presence and absence of NCNPE-AgNPs in 1.0 M HCl solution are shown in Figure 9, respectively. It is clear that the Bode plot only contains a single capacitive loop. An increase in the inhibitor concentration led to larger negative phase angle values at the intermediate frequency, as shown from the Bode phase plot. Phase angle readings became more negative as the concentration of the different inhibitors rose. This suggests that the inhibitive behavior happened due to more inhibitor molecules being adsorbed at the surface of mild steel [28-30].

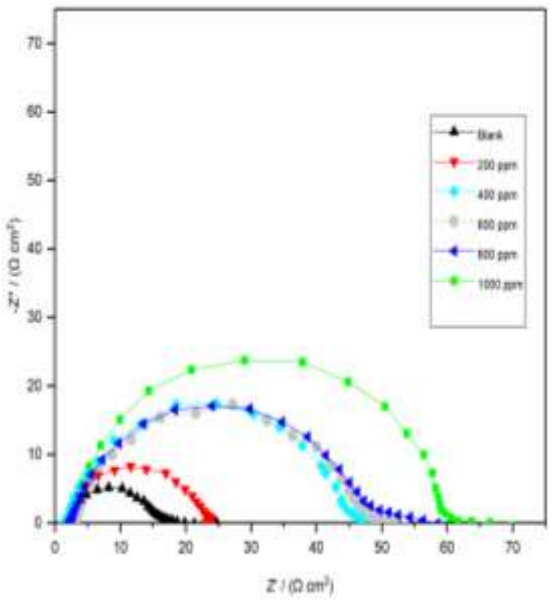

Figure 8: Nyquist plots for the CS specimen in 1.0 M HCl in the absence and presence of different concentrations of NCNPE-AgNPs

International Journal of Current Science Research and Review
ISSN: 2581-8341
Volume 08 Issue 07 July 2025
DOI: 10.47191/ijcsrr/V8-i7-02, Impact Factor: 8.048
IJCSRR @ 2025
www.ijcsrr.org

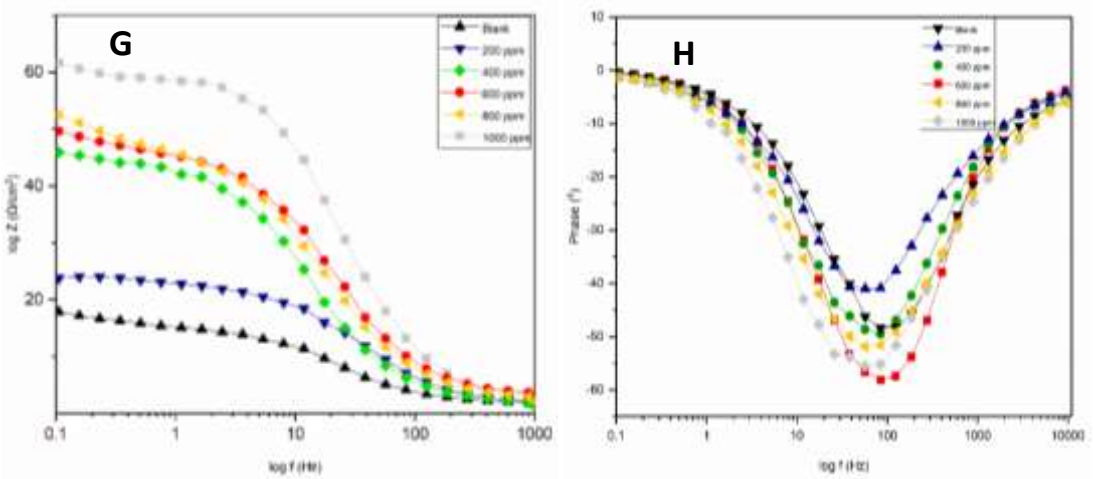

Figure 9: Bode impedance and Bode phase plots for mild steel electrode in the absence presence of NCNPE-AgNPs in 1.0 M HCl

Table 3*:* Impedance parameters for the corrosion of mild steel in 1.0 M HCl in the absence and presence of various concentrations of NCNPE-AgNPs

Concentration (ppm)	R_1 (Ω m^2)	R_2 (Ω cm^2)	R_{ct} (Ω cm^2)	C_{dl} (µF cm^{-2})	n	%IE
Blank	1.205	10.414	11.619	9.34 x 10^{-4}	0.88	-
200	1.722	25.626	27.348	7.52 x 10^{-4}	1.0	57.51
400	2.830	30.913	33.743	2.69 x 10^{-4}	0.89	65.57
600	2.610	43.304	45.914	1.33 x 10^{-4}	0.92	74.69
800	3.159	55.899	59.058	1.02 x 10^{-4}	0.86	80.33
1000	6.699	79.285	85.984	7.00 x 10^{-5}	0.87	86.49

3.2.4 Thermodynamic Consideration

The thermodynamic behaviour of the inhibitors were critically studied in order to gain insight into the mechanism of inhibition of the corrosion of mild steel in 1.0 M HCl by NCNPE-AgNPs. Thermodynamic parameters such as the energy of activation (EA), standard enthalpy (ΔH) and the entropy changes of adsorption (ΔS), were deduced through the transition state plots. The transition state equation (6) relates the corrosion rate with these thermodynamic parameters, which was further resolved to a linear expression of equation (7).

$$CR = \frac{RT}{Nh}\exp^{\left(\frac{\Delta S_{ads}}{R}\right)}\exp^{\left(\frac{-\Delta H_{ads}}{RT}\right)} \quad (6)$$

$$\log\left(\frac{CR}{T}\right) = \log\left(\frac{R}{Nh}\right) + \left(\frac{\Delta S_{ads}}{2.303R}\right) - \left(\frac{\Delta H_{ads}}{2.303RT}\right) \quad (7)$$

Figure 10a shows the Arrhenius plot for the corrosion of mild steel in 1.0 M HCl containing the various concentration of the inhibitor. The parameters deduced are recorded as **Table 4**. From the table, it can be seen that the values for the activation energy in the presence of the inhibitor are higher than in the blank. The values of the Ea also increased with increase in the inhibitor concentration for all the systems, indicating the formation of energy barrier against corrosion reaction of the CS with the HCl solution.

Figure 10b shows the transition state plots for the corrosion of mild steel in 1.0 M HCl in the absence and in the presence of the various concentration of the inhibitor. The corresponding transition state parameters obtained from the plots are recorded as

International Journal of Current Science Research and Review
ISSN: 2581-8341
Volume 08 Issue 07 July 2025
DOI: 10.47191/ijcsrr/V8-i7-02, Impact Factor: 8.048
IJCSRR @ 2025
www.ijcsrr.org

Table 5. As can be seen from the table, the values of ΔS are negative and decreased progressively with increase in the inhibitor concentration. Also, the values of ΔH obtained for all the systems are negative, the negative values increased with increase in the concentration of the inhibitor.

The negative values of entropy change of adsorption (ΔS) imply that the activation complex represents association steps and the reaction was spontaneous and feasible. Also results showed that all the enthalpy of activation (ΔH) for the inhibitors are negative, reflecting the exothermic nature of the CS dissolution process in HCl. The values of Ea shows that the NCNPE-AgNPs were physically adsorbed to the surface of the mild steel [31-32].

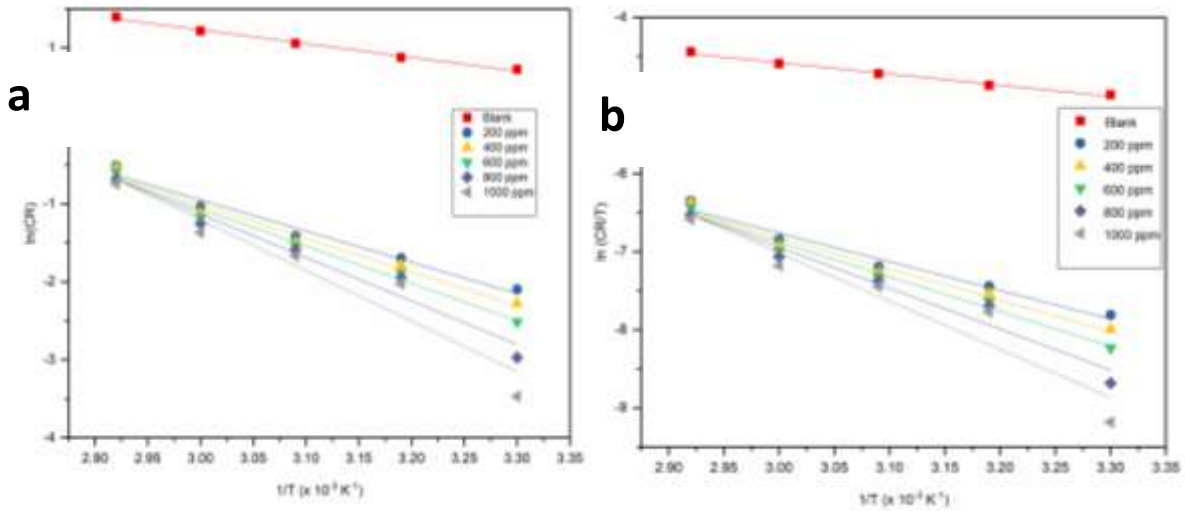

Figure 10 (a) Arrhenius and (b) Transition State plots for the corrosion of CS in 1.0 M HCl containing the various concentration of NCNPE-AgNPs

Table 4: Transition State and Arrhenius parameters for the corrosion of CS in 1.0 M HCl containing various concentration of NCNPE-AgNPs

Concentration (ppm)	ΔS^0_{ads} (J/mol)	ΔH^0_{ads} (J/mol)	Ea (J/mol)	R^2
Blank	-199.68	-11.97	14.68	0.99
200	-161.91	-30.61	33.31	0.98
400	-154.13	-33.36	36.07	0.98
600	-143.85	-36.95	39.66	0.99
800	-124.47	-43.59	46.30	0.96
1000	-101.97	-51.29	54.00	0.92

3.2.5 Adsorption Consideration

The effectiveness of organic compounds as corrosion inhibitors can be ascribed to the molecules' adsorption through their polar functions on the metal surface. Adsorption isotherm values are important to explain the mechanism of corrosion inhibition of organo-electrochemical reactions of metals and alloys [33-35]. Different adsorption isotherms were tested in order to obtain more information about the interaction between the mild steel surface and the at various temperature. The various isotherms tested includes Temkin, Frumkin, Freundlich, Flory-Huggins, and Langmuir adsorption isotherms among others. The linear regression coefficients (R^2) were used to determine the best fit. Langmuir adsorption isotherm was found to be best fit in which case the linear regression coefficients (R^2) were close to unity. Langmuir adsorption isotherm assumes that the solid surface contains a fixed number of adsorption sites and each site holds one adsorbed species, [36-38].

International Journal of Current Science Research and Review
ISSN: 2581-8341
Volume 08 Issue 07 July 2025
DOI: 10.47191/ijcsrr/V8-i7-02, Impact Factor: 8.048
IJCSRR @ 2025
www.ijcsrr.org

The Langmuir isotherm plots of log C/θ against log C for the adsorption of NCNPE-AgNPs at various temperature are shown in **Figure 11**. The equilibrium constant of adsorption of the inhibitors on the mild steel surface is related to the standard free energy of adsorption ΔG^0_{ads} by Equation 8.

$\Delta G^0 ads = -2.303RT \log (55.5Kads)$ 8

where R is the molar gas constant, T is the absolute temperature, and 55.5 is the water concentration in solution expressed in mol L^{-1} [39]. Langmuir parameters for the corrosion of mild steel in 1.0 HCl containing various concentrations of the studied inhibitors calculated from the slope and intercept of the plots are presented in **Table 5**.

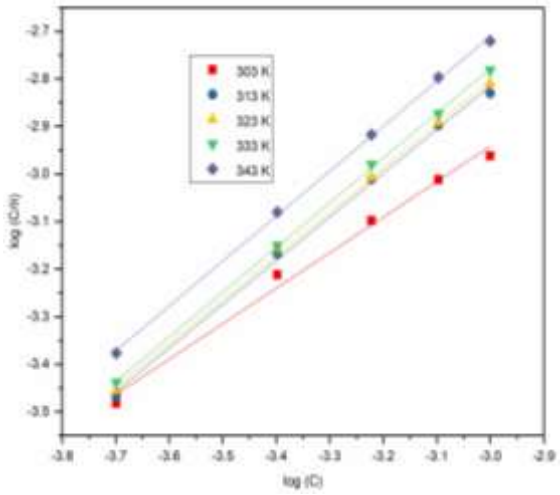

Figure 11: Langmuir isotherm for the adsorption of NCNPE-AgNPs on CS surface in 1.0 M HCl solution at various temperatures

Table 5: Langmuir parameters for the corrosion of mild steel in 1.0 HCl containing various concentrations of NCNPE-AgNPs calculated from the slope and intercept of the plots are presented in.

T (K)	Slope	Intercept	R^2	k_{ads}	ΔG^0_{ads} (kJ/mol)
303	0.7458	-0.7046	0.9907	0.1974	-6.03
313	0.919	-0.0577	0.9977	0.8756	-10.11
323	0.9221	-0.0364	0.9987	0.9196	-10.56
333	0.9393	-0.0391	0.9997	0.9139	-10.87
343	0.9447	-0.1232	0.9992	0.7530	-10.65

4. CONCLUSION

Synthesis and characterization of NCNPE-AgNPs was effectively carried out. The mean particle size of the synthesized nanoparticles was found to be 1.36128 ± 0.04962. Treatment of the face-centred cubic structured (fcc) crystalline NCNPE-AgNPs by Scherer's equation gave the average crystallite size of 2.36 nm. NCNPE-AgNPs has proven to be a good inhibitor for the corrosion of CS in HCl. The %IE using gravimetric and electrochemical impedance spectroscopy methods was found to increase to a maximum of 96.44 and 86.49 %, respectively, in the presence of 1000 ppm. The effectiveness of this inhibitor was however lowered by rise in temperature. The negative values of entropy change of adsorption (ΔS) imply that the inhibitor molecules freely moving in the bulk solution were adsorbed in an orderly fashion onto the CS surface. Also, the activation complex represents association steps and the reaction was spontaneous and feasible. Also results showed that all the enthalpy of activation (ΔH) for the inhibitors are negative, reflecting the exothermic nature of the CS dissolution process in HCl. The physically adsorbed NCNPE-AgNPs on the CS surface in HCl was found to obey Langmuir adsorption isotherm. The results of this study revealed that the NCNPE-AgNPs is a low-cost green and effective inhibitor of corrosion of CS.

International Journal of Current Science Research and Review
ISSN: 2581-8341
Volume 08 Issue 07 July 2025
DOI: 10.47191/ijcsrr/V8-i7-02, Impact Factor: 8.048
IJCSRR @ 2025
www.ijcsrr.org

REFERENCES

1. G.A. Ijuo, M. A. Orokpo, N. Surma, P.N Tor, "Methanol extract of *Canarium Sweinfurthii* as a green inhibitor for the corrosion of mild steel in HCl: adsorption, kinetic, thermodynamic and synergistic studies" J. Mater. Environ. Sci., 2018, 9, 11, 3113-3123
2. A. M. Orokpo, R. A. Wuana, H.F. Chuhul, I.S. Eneji, "Corrosion Inhibition Potential of Benue Propolis Extracts on Carbon Steel in 1.0 M Hydrochloric Acid Medium: Experimental and Computational Studies," Progress in Chemical and Biochemical Research 2022, 5, 3, 283-300
3. F. George, P.E. Hays, "International Symposium on Corrosion for Sustainable development, World Corrosion Organization, 2022.
4. L. T. Popoola, A. S. Yusuff, O. M. Ikumapayi, O. M. Chima, A. T. Ogunyemi, B. A. Obende, "Electrochemical, Isotherm, and Material Strength Studies of Cucumeropsis mannii Shell Extract on A515 Grade 70 Carbon Steel in NaCl Solution," Hindawi International Journal of Corrosion, 2022, 3189844, 22, https://doi.org/10.1155/2022/3189844
5. B. R. Fazal, T. Becker, B. Kinsella, and K. Lepkova, "A review of plant extracts as green corrosion inhibitors for CO_2 corrosion of carbon steel," npj Materials Degradation, 2022, 6.
6. A. S. Fouda1, H. S. El-Desoky, M. A. Abdel-Galeil, D. Mansour, "Niclosamide and dichlorphenamide: new and effective corrosion inhibitors for carbon steel in 1M HCl solution" SN Applied Sciences, 2021, 3, 287, https://doi.org/10.1007/s42452-021-04155-w
7. C. C. Aralu, H. O. Chukwuemeka-Okorie, K. G. Akpomie, "Inhibition and adsorption potentials of mild steel corrosion using methanol extract of *Gongronema latifoliuim*," Applied Water Science, 2021, 11, 22 https://doi.org/10.1007/s13201-020-01351-8
8. V.D. Wagh "Propolis, a wonder bees product and its pharmacological potentials" Adv Pharmacol Sci, 2013, 308249
9. G.A. Burdock, "Review of the biological properties and toxicity of bee propolis" Food and Chemical Toxicology; 1998, 36, 347–363
10. S. Patil, N. Desai, K. Mahadik, A. Paradkar, "can green synthesized propolis loaded silver nanoparticulate gel enhance wound healing caused by burns?" European Journal of Integrative Medicine, 2015, S1876-3820, 00043-8, http://dx.doi.org/10.1016/j.eujim.2015.03.002
11. D. Nayak, S. Ashe, P.R. Rauta, "Bark extract mediated green synthesis of silver nanoparticles: Evaluation of antimicrobial activity and antiproliferative response against osteosarcoma" Mater Sci Eng, 2016, 58, 44–52.
12. T.W. Quadri, L.O. Olasunkanmi, O.E. "Fayemi, Zinc oxide nanocomposites of selected polymers: synthesis, characterization, and corrosion inhibition studies on mild steel in HCl solution" ACS Omega, 2017, 2, 8421–8437.
13. M.M. Solomon, H. Gerengi, S.A. Umoren, "Gum Arabic – silver nanoparticles composite as a green anticorrosive formulation for steel corrosion in a strong acid media," Carbohyd Polym, 2018, 181, 43–55.
14. T.B. Asafa, M.O. Durowoju, K.P. Madingwaneng, S. Diouf, E.R. Sadiku, M.B Shongwe, P.A. Olubami, O.S. Ismail. M.T. Ajala and K.O. Oladosun, "Gr-Al composite reinforced with Si3N4 and SiC particles for enhanced microhardness and reduced thermal expansion," Appl. Sci. 2020, 1026. https://doi.org/10.1007/s42452-020-2838-5
15. G. A. Ijuo, S. Nguamo, J. O. Igoli, "Ag-nanoparticles Mediated by *Lonchocarpus laxiflorus Stem Bark* Extract as Anticorrosion Additive for Mild Steel in 1.0 M HCl Solution," Progress in Chemical and Biochemical Research 2022, 5, 2, 133-146
16. O.A. Odewole, C.U. Ibeji, H.O. Oluwasola, O.E. Oyeneyin, K.G. Akpomie, C.M. Ugwu, C.G. Ugwu, T.E. Bakare, "Synthesis and anti-corrosive potential of Schiff bases derived 4-nitrocinnamaldehyde for mild steel in HCl medium: experimental and DFT studies". J Mol Struct, 2021, 1223:129214
17. H. P. Meena, A. P. Singh, and K. K. Tejavath, "Biosynthesis of Silver Nanoparticles Using Cucumis prophetarum Aqueous Leaf Extract and Their Antibacterial and Antiproliferative Activity Against Cancer Cell Lines", ACS OMEGA, 2020, 2020, 5, 5520−5528, https://dx.doi.org/10.1021/acsomega.0c00155
18. K. Shameli, M. Bin Ahmad, E.A.J. Al-Mulla, N.A. Ibrahim, P. Shabanzadeh, A. Rustaiyan, Y. Abdollahi, S. Bagheri, S. Abdolmohammadi, M.S. Usman, M. Zidan, "Green biosynthesis of silver nanoparticles using Callicarpa maingayi stem," Molecules, 2016, 8506-17. doi: 10.3390/molecules17078506.
19. M. Bilal, T. Rasheed, H.M. Iqbal, C. Li, H. Hu, X. Zhang, " Development of silver nanoparticles loaded chitosan-alginate constructs with biomedical potentialities," Int. J. Biol. Macromol, 2017, 105, 393−400.

International Journal of Current Science Research and Review
ISSN: 2581-8341
Volume 08 Issue 07 July 2025
DOI: 10.47191/ijcsrr/V8-i7-02, Impact Factor: 8.048
IJCSRR @ 2025
www.ijcsrr.org

20. G. M Srirangam, K.ParameswaraRao, "Synthesis and charcterization of silver nanoparticles from the leaf extract of Malachra capitata (L.)," RJC, 2017, 10, 1, 46-53
21. V. Thiruvengadam, A.V. Bansod, "Characterization of Silver Nanoparticles Synthesized using Chemical Method and its Antibacterial Property," Biointerface Research in Applied Chemistry, 2020, 10, 6, 10.33263/BRIAC106.72577264
22. P. Logeswari, S. Silambarasan, J. Abraham, " Synthesis of silver nanoparticles using plants extract and analysis of their antimicrobial property," J Saudi Chem Soc, 2015, 19:311–317.
23. L. S. Al Banna, N. M. Salem, G. A. Jaleel and A. M. Awwad, "Green synthesis of sulfur nanoparticles using Rosmarinus officinalis javanica leaves extract and nematicidal activity against Meloidogyne," Chemistry International, 2020, 6, 3
24. J. Liu, "Advances and Applications of Atomic-Resolution Scanning Transmission Electron Microscopy," Microscopy and Microanalysis 2021, 27, 943–995 doi:10.1017/S1431927621012125
25. S. V. Kalinin, C. Ophus, P. M. Voyles, R. Erni, D. Kepaptsoglou, V. Grillo, A. R. Lupini, M. P. Oxley, E. Schwenker, M. K. Y. Chan, J. Etheridge, X. Li, G. G. D. Han, M. Ziatdinov, N. Shibata, S. J. Pennycook, "Machine learning in scanning transmission electron microscopy," Nature Reviews Methods Primers, 2022, 2, 1, 10.1038/s43586-022-00095-w
26. V.O. Kharlamov, Aleksandr Vasilevich Krokhalev, S.V. Kuz'min, V.I. ysak, "Investigation of the Structure and Distribution of Chemical Elements between the Phases of Hard Alloys of the Cr_3C_2-Ti System, Obtained at Various Modes of Explosive Compaction," Materials Science Forum, 2020, 992, 487-492, 10.4028/www.scientific.net/MSF.992.487.
27. G. A. Ijuo, A. M. Orokpo, P. N. Tor, "Effect of *Spondias mombin* Extract on the Corrosion of Mild Steel in Acid Media," *Chemistry Research Journal*, 2018, 3, 3, 64-77
28. A. M. Orokpo, R. A. Wuana, H.F. Chuhul, I.S. Eneji, "Corrosion Inhibition Potential of Benue Propolis Extracts on Carbon Steel in 1.0 M Hydrochloric Acid Medium: Experimental and Computational Studies," Progress in Chemical and Biochemical Research 2022, 5, 3, 283-300
29. E. Ituen, L. Yuanhua, C. Verma, A. Alfantazi, O. Akaranta, E. E. Ebenso, ''Synthesis and characterization of walnut husk extract-silver nanocomposites for removal of heavy metals from petroleum wastewater and its consequences on pipework steel corrosion,'' Journal of Molecular Liquids, 2021, 335, 116132, doi.org/10.1016/j.molliq.2021.116132.
30. H.F.Chahul, C.O. Akalezi, A.M. Ayuba, "Effect of adenine, guanine and hypoxanthine on the corrosion of mild steel in H3PO4. International Journal of Chemical Science," 2015, 7, 2006-3350.
31. A. Akpan, N.O. Offiong, "Electrochemical linear polarization studies of Amodiaquine drug as a corrosion inhibitor for mild steel in 0.1M HCl solution," Chem Mater Res, 2015, 7, 17–20
32. M. H. Nazari, M. S. Shihab, L. Cao, E. A. Havens, and X. Shi, "A peony-leaves-derived liquid corrosion inhibitor: protecting carbon steel from NaCl," Green Chemistry Letters and Reviews, 2017, 10, 4, 359–379.
33. M. H. Nazari, M. S. Shihab, E. A. Havens, and X. Shi, "Mechanism of corrosion protection in chloride solution by an applebased green inhibitor: experimental and theoretical studies," Journal of Infrastructure Preservation and Resilience, 2020, 1, 7.
34. N. B. Iroha, N. J. Maduelosi, "Corrosion Inhibitive Action and Adsorption Behaviour of *Justicia Secunda* Leaves Extract as an Eco-Friendly Inhibitor for Aluminium in Acidic Media" 2021, 11, 13019 – 13030, doi.org/10.33263/BRIAC115.1301913030
35. A.I. Ali, Y.S. Mahrousb, "Corrosion inhibition of C-steel in acidic media from fruiting bodies of Melia azedarach L extract and a synergistic Ni^{2+} additive", RSC Adv. 2017, 7, 23687–23698
36. N.AI Otaibi, H.H. Hammud, Corrosion Inhibition Using Harmal Leaf Extract as an Eco-Friendly Corrosion Inhibitor, Molecules, 26(2021) 7024, https://doi.org/10.3390/molecules26227024
37. G.A. Ijuo, H.F. Chahul, and I.S. Eneji, Corrosion inhibition and adsorption behavior of Lonchocarpus laxiflorus extract on mild steel in hydrochloric acid. Ew J Chem Kinet 2016, 1, 21-30.
38. S. Ibrahim, R. Sanmugapriya, J. A. Selvi, T. P. Malini, P. Kamaraj, P. A. Vivekanand,G. Periyasami, A. Aldalbahi, K. Perumal, J. Madhavan, and S. Khanal, **"**Effect of 3-Nitroacetophenone on Corrosion Inhibition of Mild Steel in Acidic Medium," 2022, 2022, https://doi.org/10.1155/2022/7276670

Cite this Article: Ijuo, G.A., Ukoha, P.O., Surma, N. (2025). Biosynthesis of Ag-nanoparticles from North Central Nigerian Propolis Extract as Highly Efficient Anticorrosion Additive of Carbon Steel in Acidic Medium. International Journal of Current Science Research and Review, 8(7), pp. 3166-3177. DOI: https://doi.org/10.47191/ijcsrr/V8-i7-02